RECENT DEVELOPMENTS IN NANOSECOND PULSED SLIDING DISCHARGE FOR AIRFLOW CONTROL

K. D. BAYODA*[1], N. BENARD[1], E. MOREAU[1]

[1]*Institut PPRIME (CNRS UPR 3346, Université de Poitiers, ISAE-ENSMA)*
SP2MI - Téléport2 Bd Marie & Pierre Curie BP 30179, 86962 Futuroscope, France.
*Corresponding author's e-mail: kossi.bayoda@univ-poitiers.fr

ABSTRACT

This study characterizes a sliding discharge based on a three-electrode geometry supplied simultaneously by a nanosecond repetitive pulse high voltage and a DC high voltage. It proposes iCCD visualizations of the discharge propagation and a detailed explanation of the associated electrical quantities (voltage, current, power and consumed energy).

1. INTRODUCTION

Surface DBD and corona discharges have been widely studied this last decade for their numerous applications in aerodynamic flow control by plasma actuators [1]. On one hand, surface DBD supplied by an ac sine high voltage produces an electric wind based wall jet. On the other hand, if the high voltage has a nanosecond repetitively pulsed waveform, the sudden gas heating at the dielectric wall results in a pressure wave [2]. Both mechanical phenomena can interact with incoming airflow in order to control it. However, with a two-electrode geometry, the discharge extension along the dielectric wall is limited to a few mm. A way to increase the area of the surface discharge is to use a second air-exposed electrode, located in front of the high voltage one [3-6]. Visualizations with exposure time of a few seconds have shown that the nanosecond sliding discharge can cover the whole area between both air-exposed electrodes [6].
The goal of the present paper is to complete these previous works by investigating the filament development in both discharges, with the help of iCCD visualizations. Electrical measurements are also provided to highlight the behavior of this discharge.

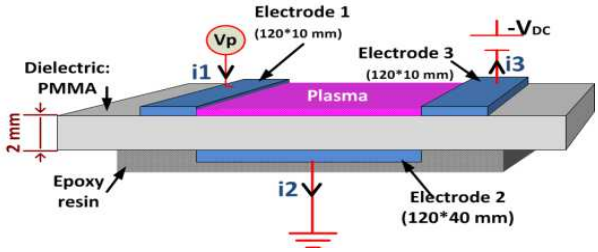

Fig. 1: Sliding discharge actuator.

2. SETUP

The plasma actuator is made of three aluminum foil electrodes flush-mounted on a PMMA flat plate as described in Fig. 1. To ignite a typical nanosecond pulsed DBD, a positive pulsed high voltage V_P is applied between the first air-exposed electrode (1) and the grounded one (2), with the help of a FID power supply (model FPG 40-30NK, 30 kV_{max}, 35 mJ). Pulse voltage is measured by a NorthStar probe (model PVM-1, 400 MHz). The pulse frequency is triggered at 1 kHz with a delay generator Stanford (model DG645 645). To establish the sliding DBD, a negative dc high voltage $-V_{DC}$ is applied at the second air-exposed electrode (3) with a dc power supply (SPELLMAN, -40 kV, 150 W). The system is optimized to minimize the perturbations and reflected pulses. To determine the energy released by every power supply, two currents i_1 and i_3 are measured respectively on electrodes 1 and 3 using current transformers (Bergoz CT-D5.0 and CT-D1.0) with respectively a bandwidth of 400 MHz and 500 MHz. These currents were synchronized with a non-inductive resistance to avoid time delay between voltage and current measurements, in order to cancel error on the energy computation. All the signals are recorded by a WaveRuner oscilloscope (204 mxi 2 GHz). This work presents results for pulsed voltage peak V_P fixed at 15 kV_p and several negative DC high voltages $-V_{DC}$ (0, -16, -20 kV_{DC}).

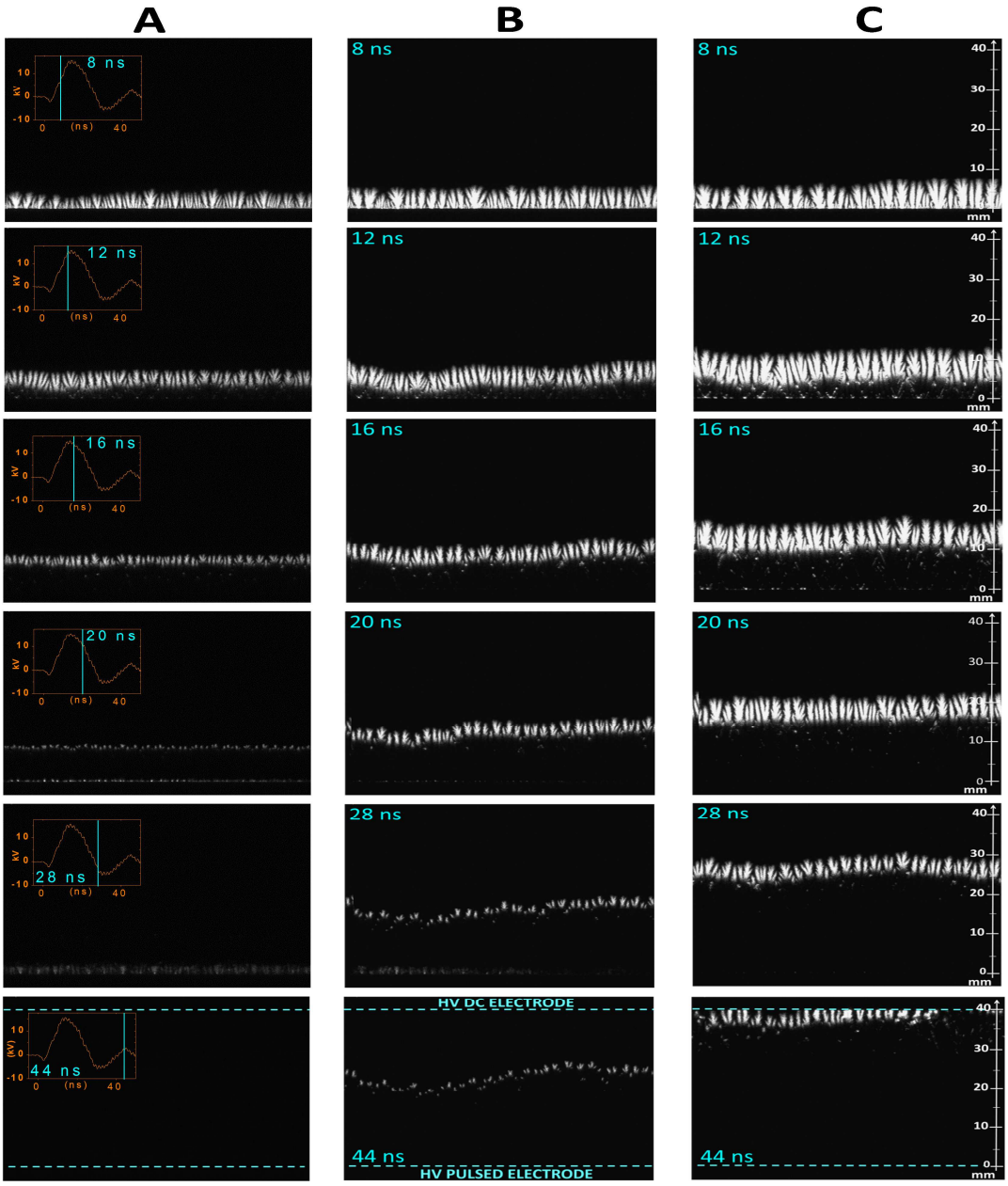

Fig. 2: Front iCCD visualisations of the discharge evolution during 44 ns for a single DBD discharge (A: V_P = 15 kV_p and V_{DC} = 0 kV_{DC}) and a sliding discharge : (B: V_P = 15 kV_p and V_{DC} = 16 KV_{Dc}) and (C: V_P = 15 kV_p and V_{DC} = 20 kV_{DC})

The plasma images are taken by an iCCD camera (PI-MAX-1024i) coupled with an UV lens (100F/2.8). The exposure time is 4 ns. A total of 25 images of 1024x800 pixels² are considered in order to observe the filaments development on the dielectric surface.

3. SLIDING PLASMA ICCD IMAGES

Figure 2 show the discharge propagation during one cycle. The *Fig. 2-A* presents a typical single DBD in a two-electrode configuration because the potential of electrode (3) is 0 kV. These images reveal that once the discharge is ignited (t = 8 ns), the filaments are formed from the high voltage electrode (located at the bottom of the images) and propagate up to 13 mm at t = 16 ns. Before their extinction, secondary thin ionization channels of lower intensity occur at the electrode edge (t = 20 to 28 ns).

When a DC voltage is applied to the third electrode, the ionized channels extend further than with a typical single nanosecond DBD. When a DC high voltage of -16 kV is applied to the second air-exposed electrode (*Fig. 2-B*), the filaments extend up to 25 mm. By increasing the DC voltage to -20 kV (*Fig. 2-C*), the discharge extend further and reach electrode (3). A sliding

discharge occurs. In this condition, the filaments are stuck to the dc electrode (3). This can be explained by the work function of the aluminum electrode (4.25 eV) [7] and the recombined effect of ions with electrons provided by the DC supply. These images reveal that the intensity, the length and the propagation velocity of the ionized channels increase with the electric field generated at the dielectric surface by the dc voltage component.

4. ELECTRICAL MEASUREMENTS

4-. 1 CURRENT MEASUREMENTS

Figure 3 shows electrical measurements corresponding to the iCCD images shown previously. *Fig. 3-A* shows the voltage pulse waveform and the current i_1 measured on the first electrode for three V_{DC} values. The nanosecond pulse rising and decaying times are equal to about 1 ns/kV and the pulse width is around 20 ns. *Fig. 3-B* presents the currents measured on the third electrode for the same three cases. For V_{DC} = 0 kV, a typical nanosecond DBD current is measured on the first electrode and no current is observed on the opposite electrode (3). By varying the DC voltage at the third electrode, for a pulsed voltage V_P fixed at 15 kV_p, no significant changes have been observed on both currents (i_1 and i_3) until V_{DC} is smaller than 14 kV. When V_{DC} > 14 kV, both currents i_1 and i_3 increase (*Fig. 3 A and B* for V_{DC} = 16 kV and 20 kV). This augmentation highlights the effect of the electric field on the ionized channels, their length and the velocity of the electronics species. First, the current i_3 starts earlier for V_{DC} = 20 kV (t = 30 ns) than for V_{DC} = 16 kV (t = 40 ns), showing that the ionized channels propagate faster when V_{DC} is increased. Moreover, its peak value and its duration are higher, traducing a more intense discharge.

4-. 2 POWER AND ENERGY

$$P_{total}(t) = [v_p(t) * i_1(t)] + [v_{dc}(t) * i_3(t)] \quad (*)$$
$$E_{total}(t) = \int P_{total}(t)\, dt \quad (**)$$

The instantaneous power consumed by the discharge is computed with equation (*), as the addition of the power provided by both pulsed and DC power supplies. The *Fig. 3-C* plots instantaneous power consumption of the discharge. It shows that the maximum power peak is released by the pulsed part. As for the current, it was observed that the power does not vary significantly until V_{DC} = 14 kV .

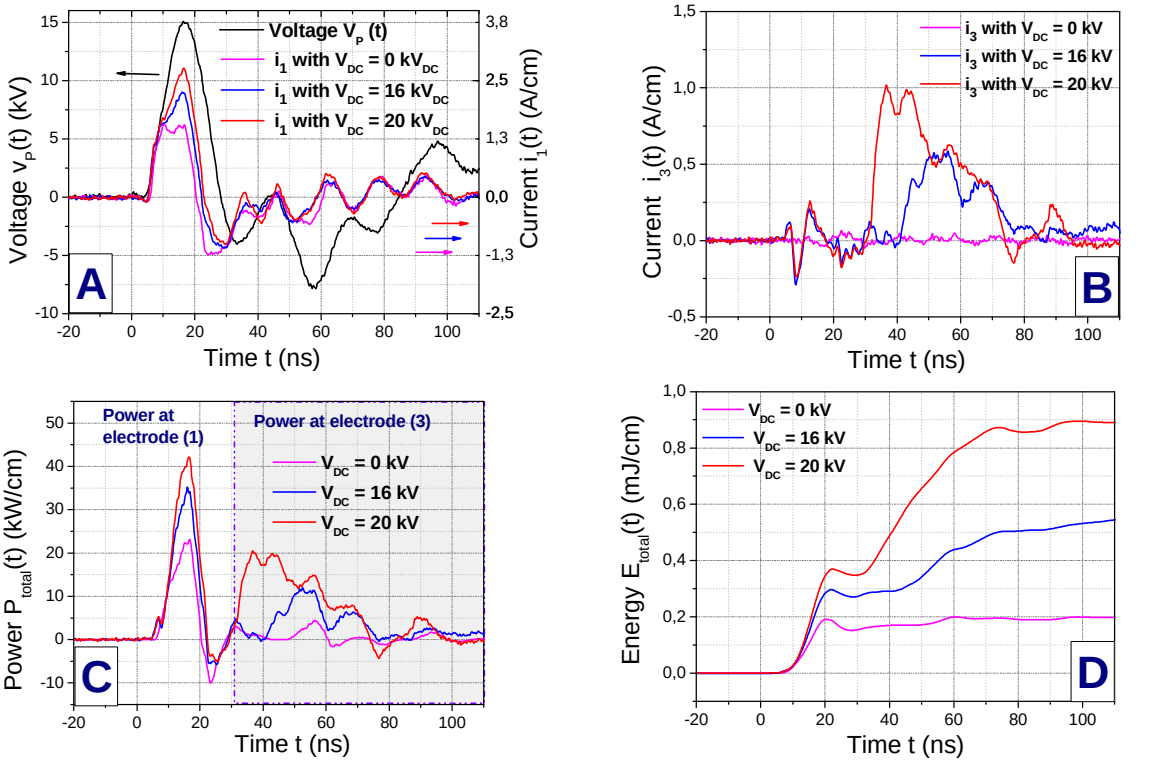

Fig. 3: Electrical measurements versus time (A: pulsed voltage and current on electrode (1); B: current on electrode (3); C: consumed power; D: total energy).

The total energy is computed by integrating the total power as in equation (**). The *Fig.3-D* shows energy versus time. At V_{DC} = 0 kV, energy corresponds to the one consumed by a single two-electrode nanosecond DBD (0.20 mJ/cm). For V_{DC} = 16 kV and 20 kV, the total energy strongly increases (up to 0.56 and 0.90 mJ/cm). Although the maximum power peak is released by the pulsed part, the most energy is provided by the DC power supply due to the higher duration of current i_3 (see *Fig. 3-B*). However, adding a DC component does not affect systematically the total energy. In fact, it seems that the main parameter that results in the energy augmentation is the surface potential difference V_{PD} between both air-exposed electrode, *i.e.* V_P minus V_{DC}. To illustrate that, Fig. 4 shows the energy as a function of this potential difference, for V_P = 10, 13 and 15 kV_p. In this figure, the energy provided by only the pulse high voltage power supply is plotted with open symbols when the total energy is represented with closed symbols. On one hand, if one consider only the energy provided by the pulse HV, one can see that this one increases monotoneously with V_{PD}. On the other hand, for the three V_P values, the total energy rises when V_{PD} reaches 27 kV, whatever the V_P value, showing that the sliding discharge is ignited when V_{PD} exceeds a given threshold.

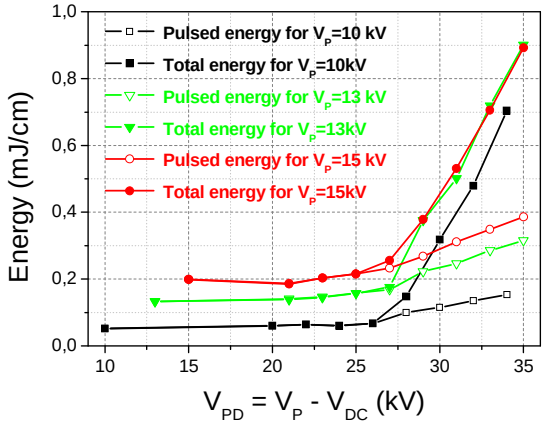

Fig. 4: Energy as a function of the potential difference between both air-exposed electrodes (V_P – V_{DC}) for three values of V_P.

5. CONCLUSION AND PERSPECTIVES

This work provides optical and electrical characterization of a nanosecond pulsed sliding discharge. It confirms that adding a DC component to a typical nanosecond DBD has an impact on the ionization channels and the electrical properties. By removing the accumulated surface charges that are collected by the DC air-exposed electrode, the sliding actuator promises to be interesting for flow control. Furthermore, Schlieren vizualisations (not shown in the present paper) of the pressure wave produced by the sliding discharge showed that this one is strongly modified compared to the one induced by a single DBD.

6. ACKNOWLEDGMENTS

This work was funded by the French Government program “Investissements d’Avenir” (LABEX INTERACTIFS, reference ANR-11-LABX-0017-01) and partially funded by DGA and ANR INOPLAS.

REFERENCES

[1]. E. Moreau, "Airflow control by non-thermal plasma actuators." J. phys. D. Appl. Phys **40** 605-636, 2007.

[2]. N. Benard, N. Zouzou, A. Claverie, J. Sotton, E. Moreau, “Optical visualization and electrical characterization of fast-rising pulsed dielectric barrier discharge for airflow control applications”, Journal of Applied Physics, **111**, 2012.

[3]. E. Moreau, R. Sosa, G. Artana, « Electric wind produced by surface plasma actuators: a new dielectric barrier discharge based on a three-electrode geometry”, Journal of Physics D: Applied Physics, **41**, 2008.

[4]. C. Louste, G. Artana, E. Moreau, and G. Touchard. "Sliding discharge in air at atmospheric pressure: electrical properties." journal of electrostatics, **63**, 615-620, 2005.

[5]. k. Takashima, N. Zouzou, E. Moreau, A. Mizuno, G. Touchard. "Generation of extended surface barrier discharge on dielectric surface -electrical properties", Plasma environmental science and technology **1** 14-20, 2007.

[6]. R. Sosa, H. Kelly, D. Grondona, A. Marquez, V. Lago, and G. Artana. "Electrical and plasma characteristics of a quasi-steady sliding discharge." J. Phys. D: Appl. Phys. **41**, 035202, 2008.

[7]. H. M. Song, M. Jia, H. Liang, and Y. Wu. "Experimental investigation of the plasma aerodynamic actuation generated by nanosecond-pulsed sliding discharge", IEEE. 3rd International conference on measuring technology and mechatronics automation. Shanghai, 116-119, 2011.